Available online at www.sciencedirect.com
ScienceDirect
Geochimica et Cosmochimica Acta 71 (2007) 2224–2239
Geochimica et Cosmochimica Acta
www.elsevier.com/locate/gca

Characterization of elemental release during microbe–basalt interactions at $T = 28$ °C

Lingling Wu [a,*], Andrew D. Jacobson [a], Hsin-Chieh Chen [b], Martina Hausner [b]

[a] Department of Earth and Planetary Sciences, Northwestern University, 1850 Campus Drive, Evanston, IL 60208-2150, USA
[b] Department of Civil and Environmental Engineering, Northwestern University, 2145 Sheridan Road, Evanston, IL 60208, USA

Received 3 October 2006; accepted in revised form 27 February 2007; available online 6 March 2007

Abstract

This study used batch reactors to characterize the rates and mechanisms of elemental release during the interaction of a single bacterial species (*Burkholderia fungorum*) with Columbia River Flood Basalt at $T = 28$ °C for 36 days. We primarily examined the release of Ca, Mg, P, Si, and Sr under a variety of biotic and abiotic conditions with the aim of evaluating how actively metabolizing bacteria might influence basalt weathering on the continents. Four days after inoculating *P-limited* reactors (those lacking P in the growth medium), the concentration of viable planktonic cells increased from $\sim 10^4$ to 10^8 CFU (Colony Forming Units)/mL, pH decreased from ~7 to 4, and glucose decreased from ~1200 to 0 μmol/L. Mass-balance and acid–base equilibria calculations suggest that the lowered pH resulted from either respired CO_2, organic acids released during biomass synthesis, or H^+ extrusion during NH_4^+ uptake. Between days 4 and 36, cell numbers remained constant at $\sim 10^8$ CFU/mL and pH increased to ~5. Purely abiotic control reactors as well as control reactors containing inert cells ($\sim 10^8$ CFU/mL) showed constant glucose concentrations, thus confirming the absence of biological activity in these experiments. The pH of all control reactors remained near-neutral, except for one experiment where the pH was initially adjusted to 4 but rapidly rose to 7 within 2 days. Over the entire 36 day period, *P-limited* reactors containing viable bacteria yielded the highest Ca, Mg, Si, and Sr release rates. Release rates inversely correlate with pH, indicating that proton-promoted dissolution was the dominant reaction mechanism. Both biotic and abiotic *P-limited* reactors displayed low P concentrations. Chemical analyses of bacteria collected at the end of the experiments, combined with mass-balances between the biological and fluid phases, demonstrate that the absence of dissolved P in the biotic reactors resulted from microbial P uptake. The only P source in the basalt is a small amount of apatite (~1.2%), which occurs as needles within feldspar grains and glass. We therefore conclude that *B. fungorum* utilized apatite as a P source for biomass synthesis, which stimulated elemental release from coexisting mineral phases via pH lowering. The results of this study suggest that actively metabolizing bacteria have the potential to influence elemental release from basalt in continental settings.

1. INTRODUCTION

Numerous field and laboratory investigations have focused on basalt weathering, owing to its important role in the regulation of river, seawater, and soil geochemistry as well as the long-term evolution of Earth's climate (e.g., Gislason and Eugster, 1987a,b; Bluth and Kump, 1994; Brady and Gislason, 1997; Chadwick et al., 1999, 2003; Taylor and Lasaga, 1999; Vitousek et al., 1999; Dessert et al., 2001, 2003; Oelkers and Schott, 2001; Stewart et al., 2001; Dupré et al., 2003; Pokrovsky et al., 2005; Das et al., 2006; Wolff-Boenisch et al., 2006). These studies have revealed much about basalt dissolution and its primary controls, although largely from an inorganic perspective. Less is known about biologically mediated basalt weathering. A few investigations have examined the influence of vascular plants, organic acids, and ligands (e.g., Drever, 1994; Cochran and Berner, 1996; Drever and Stillings, 1997; Moulton

* Corresponding author. Fax: +1 847 491 8060.
E-mail address: lingling@earth.northwestern.edu (L. Wu).

0016-7037/$ - see front matter © 2007 Elsevier Ltd. All rights reserved.
doi:10.1016/j.gca.2007.02.017

and Berner, 1998; Oelkers and Schott, 1998; Brady et al., 1999; Moulton et al., 2000; Oelkers and Gislason, 2001; Neaman et al., 2005), and there is a growing literature concerning the microbial alteration of seafloor basalt (e.g., Thorseth et al., 1992, 1995; Staudigel et al., 1995, 1998; Fisk et al., 1998; Torsvik et al., 1998; Reysenbach and Shock, 2002; Edwards et al., 2003; Daughney et al., 2004; Aouad et al., 2006; Bach et al., 2006). However, very few studies have explicitly considered how and to what extent actively metabolizing bacteria influence basalt weathering on the continents.

Recent research has demonstrated that microorganisms can accelerate elemental release from geologic materials, either directly through the acquisition of limiting nutrients required for biomass synthesis (e.g., P and Fe) (Rogers et al., 1998; Kalinowski et al., 2000; Bennett et al., 2001; Welch et al., 2002) or indirectly through the release of exoproducts that lower pH, complex cations, and/or change mineral saturation states (Vandevivere et al., 1994; Ullman et al., 1996; Barker et al., 1998; Liermann et al., 2000). In contrast, other work has shown that microbial activities can inhibit elemental release by facilitating development of an amorphous leached layer (Benzerara et al., 2004, 2005), promoting adsorption of polysaccharides onto mineral surfaces (Welch et al., 1999), preventing formation of etch-pits (Lüttge and Conrad, 2004), and releasing ferric iron that interacts with surface sites (Santelli et al., 2001; Welch and Banfield, 2002). Thus, an underlying motivation for this study was to help resolve whether actively metabolizing bacteria either enhance or inhibit elemental release from silicate minerals. We specifically focused on basalt because it is an abundant reservoir of P and Fe relative to other crustal rocks (e.g., Li, 2000; Wolff-Boenisch et al., 2004). It therefore follows that basalt could be a convenient source of limiting nutrients required for microbial growth, which could have important consequences for elemental release compared to purely abiotic conditions.

To test this hypothesis, we characterized the rates and mechanisms of elemental release during microbe–basalt interactions under laboratory-scale conditions nominally representative of some terrestrial environments (e.g., tropical watersheds). We primarily examined major elements involved in the carbonate-silicate geochemical cycle (Ca, Mg, and Si), life-supporting nutrients (P), and trace elements (Sr) whose isotope composition ($^{87}Sr/^{86}Sr$) is used as a proxy for chemical weathering processes (e.g., Taylor and Lasaga, 1999; Berner and Kothavala, 2001; Dessert et al., 2001; Das et al., 2006; Lerman and Wu, in press). Although the idea that microbes can influence basalt weathering is not new (Staudigel et al., 1995, 1998; Daughney et al., 2004), this study quantifies for the first time the release of the aforementioned elements during microbe–basalt interactions at the whole-rock scale. The data reveal that the bacterium studied (*Burkholderia fungorum*) accelerates elemental release through pH lowering. Within this context, our findings imply that microbe–basalt interactions have the potential to influence a variety of Earth surface phenomena ranging from the evolution of atmospheric CO_2 (e.g., Berner and Kothavala, 2001) to base cation cycling during basaltic soil formation (e.g., Vitousek et al., 1999; Chadwick et al., 2003).

2. MATERIALS AND METHODS

2.1. Characterization and preparation of basalt samples

Samples of the Columbia River Flood Basalt (CRFB) were purchased from Ward's Scientific (Product # 47E 1043). The bulk rock chemistry was determined by ActLabs in Ontario, Canada. Samples were digested by fusion with $LiBO_2$, and major and trace element concentrations were measured by ICP-OES and ICP-MS, respectively. Repeated analyses of NIST 1633b yielded an external reproducibility better than 2%.

Polished thin sections for microscopic analyses were prepared by Mineral Optics Laboratory in Wilder, VT. The elemental composition and relative abundances of minerals comprising the basalt were determined by the GeoAnalytical Laboratory at Washington State University in Pullman, WA using a Cameca Instruments electron microprobe following standard procedures. The volume proportions of major rock-forming minerals were estimated by a point counting procedure, where 441 points were analyzed in a 4×4 mm square in the middle of the thin section.

Basalt samples were broken with a hammer, and fresh pieces devoid of visible weathering rinds were crushed in a shatter box equipped with a tungsten carbide grinding container. The crushed rock was wet sieved to isolate the 45–850 μm size fraction. To remove fine particles resulting from the crushing process, the sieved samples were repeatedly ultrasonicated in MilliQ water and dried at $T = 60$ °C. No fines were observed when the cleaned particles were subsequently examined by SEM. The multi-point BET (Brunauer, Emmett and Teller)-N_2 specific surface area of the particles (5.57 m^2/g) was determined by Quantachrome Instruments in Boynton Beach, FL.

2.2. Growth media

The objective of this study was to examine how bacteria influence the release of base cations and other elements (e.g., Sr, P, and Si) from basalt when they are forced to acquire P from the rock matrix. Standard growth media typically lack Si, and it is not difficult to eliminate additives that contain P. However, most formulae yield media with very high base cation concentrations that could potentially mask the effects of rock dissolution. To circumvent this problem, we developed a specially formulated medium that primarily contains C and N required for cell growth but entirely lacks Ca and Fe and has minimal amounts of Mg, Na, and K.

The idealized formula is provided here, and bulk chemical analyses are presented in Section 3. Per liter of solution, the major constituents are glucose (0.2 g), NH_4Cl (0.04 g), KCl (0.0005 g), and $MgSO_4$ (0.0005 g), and the minor constituents are $MnCl_2 \cdot 4H_2O$ (12 μg), $CoCl_2 \cdot 6H_2O$ (4.8 μg), $CuSO_4$ (1.2 μg), $Na_2MoO_4 \cdot 2H_2O$ (3.6 μg), $ZnCl_2$ (2.4 μg), LiCl (0.6 μg), H_3BO_3 (1.2 μg), KBr (2.4 μg), KI (2.4 μg) and $BaCl_2$ (0.6 μg). Hereafter, this formula is referred to as the *P-limited medium*. According to Geochemist's Workbench, the *P-limited medium* has a low ionic strength of 0.0008 mol/L. For experiments where P was not a limiting nutrient, either 0.3 g of NaH_2PO_4 or 0.03 g of KH_2PO_4 were added per liter of solution. Hereafter, these formulae are referred to as the *P-bearing media*. These media have ionic strengths of 0.035 and 0.0035 mol/L, respectively. All media were prepared using MilliQ water, and when possible, high-purity reagents. All media were adjusted to pH 7 using ammonium hydroxide and were sterilized in pyrex glassware by autoclaving prior to use. Although the media were prepared in glassware, the release of Si from glassware during autoclaving was negligible, as evidenced from the chemical analyses presented in Table 2.

2.3. Model microorganism

The experiments were conducted using *Burkholderia fungorum*, a rod-shaped Gram-negative microorganism available from the American Type Culture Collection (ATCC #BAA-463) (Coenye et al., 2001). *B. fungorum* is a novel member of the *Burkholderia cepacia* complex. As such, considerable effort is now being directed towards characterizing its ecological and physiological properties. Recent work has identified *B. fungorum* in association with basalt comprising the Snake River Plain, Idaho (Sebat et al., 2003) and young (42–300 yr) Hawaiian volcanic deposits (Dunfield and King, 2005). *B. cepacia* has the ability to solubilize mineral-bound phosphate (Babu-Khan et al., 1995) and precipitate metal phosphate (Templeton et al., 2003). It is reasonable to assume that *B. fungorum* has similar capabilities since *B. cepacia* and *B. fungorum* belong to the same genus and can be isolated from similar environments.

2.4. Culture preparation

Prior to initiating the batch experiments described in Section 2.5, the bacteria were preconditioned in the presence of sterilized basalt particles. To sterilize the particles, 1-g samples were mixed with 5 mL of 6.15% NaOCl for 1 h in sterile 250 mL polycarbonate Erlenmeyer culture flasks with leak proof caps, washed five times with 50 mL of MilliQ water, and autoclaved in 1 mL of MilliQ for 1.5 h. The sterilized particles were then resuspended in 100 mL of *P-bearing medium*. One milliliter of the culture suspended in an optimal growth medium (Difco nutrient broth) was extracted and centrifuged at 5000 rpm for 5 min. After discarding the supernatant, 1 mL of *P-bearing medium* was added, the mixture was vortexed and centrifuged, and the supernatant was again discarded. This step was repeated three times. The resulting cell pellet was resuspended in 1 mL of *P-bearing medium*, and the optical density of the mixture was measured at 600 nm using a Spectronic 20 Genesys spectrophotometer. The washed culture was added to the flasks containing the sterilized particles and was incubated at $T = 28$ °C for 3 days. Conventional plate counting techniques showed that the initial cell density was $\sim 10^4$–10^5 CFU (Colony Forming Units)/mL.

To prepare the inoculum for the batch experiments, 80 mL of the preconditioned culture were extracted and centrifuged at 5000 rpm for 10 min. The cell pellet was washed three times with 20 mL of *P-limited medium* as described previously. Based on optical density measurements of the final suspension, 100 μL was added to the batch reactors described in Section 2.5 in order to achieve an initial cell density of $\sim 10^5$ CFU/mL.

2.5. Batch experiments

Sterile 250 mL polycarbonate Erlenmeyer culture flasks with vented caps (0.22 μm PTFE membranes) were used for the batch experiments. All elemental release experiments were conducted using a fluid:rock mass ratio of 100 or alternatively, a fluid volume:rock area ratio of 18 mL/m^2 (200 mL fluid: 2 g sterilized basalt with a BET surface area of 5.57 m^2/g).

Four elemental release experiments involving viable bacteria were conducted: B1 (bacteria + *P-limited medium*), B2 (bacteria + *P-limited medium*), B3 (bacteria + *P-bearing medium with* NaH_2PO_4), and B4 (bacteria + *P-bearing medium with* KH_2PO_4). The two reactors with *P-limited medium* (B1 and B2) can be viewed as duplicate reactors due to their identical experimental conditions. The reactors were incubated on a shaker table at $T = 28$ °C for 36 days. At 1–7 day intervals, 10.3 mL aliquots were collected with sterile serological pipettes and transferred to acid-cleaned 30-mL LDPE bottles. Each 10.3 mL aliquot was immediately processed as follows: 10 mL was passed through a 0.2 μm nylon syringe filter for concentration and pH measurements, 200 μL was similarly filtered for glucose measurements, and 100 μL was left unfiltered for plate counting.

To further constrain the importance of P limitation with respect to bacterial growth, we conducted two additional experiments in the absence of basalt: B5 (bacteria + *P-limited medium*) and B6 (bacteria + *P-bearing medium with* KH_2PO_4). The reactors were inoculated in the same manner as described above. The initial cell density in each reactor after inoculation was $\sim 10^5$ CFU/mL. The reactors were incubated on a shaker table at $T = 28$ °C for 36 days. An unfiltered 100 μL sample was collected for plate counting at 1–7 day intervals.

Five control experiments were conducted: C1 (*P-limited medium*), C2 (nonviable cells + *P-limited medium*), C3 (*P-bearing medium with* NaH_2PO_4), C4 (*P-bearing medium with* KH_2PO_4), and C5 (*P-limited medium* with initial pH adjusted to 4 with ultrapure HCl). Experiment C2 was designed to test the importance of cell wall-solute interactions on elemental release in the absence of metabolic activity. To simulate the stationary phase of the biotic reactors, a final cell density of $\sim 10^8$ CFU/mL was adopted. Approximately 100 mL was extracted from an optimal medium suspension containing $\sim 10^9$ CFU/mL cells. The sample was autoclaved and centrifuged. The resulting cell pellet was washed three times with 20 mL of *P-limited medium* and was resuspended in 100 mL of *P-limited medium*. After vortexing, the mixture was added to a reactor containing 100 mL of *P-limited medium* and 2 g of sterilized particles. Experiment C5 was designed to test the importance of low pH on elemental release. The experiment was terminated after two days, when the reactor solution reached pH 7. Samples from all control reactors were extracted and processed in a manner identical to the biological experiments.

2.6. Collection and preparation of cell biomass for chemical analyses

On day 36, the remaining fluid in reactors B1 and B2 (~85 mL) was collected to measure intracellular elemental concentrations. The liquid samples were weighed, and centrifuged at 10,000 rpm for 20 min. The cell pellet was washed with MilliQ water three times and dried at $T = 60$ °C. The dried biomass was completely digested in concentrated ultrapure HNO_3, and the resulting solutions were passed through 0.2 μm nylon syringe filters, dried, and redissolved in 5% HNO_3.

2.7. Chemical analyses

pH was measured with a VWR benchtop meter (Model #8100) and a VWR sympHony Gel 3-in-1 electrode with an uncertainty of ±0.01 pH units. Glucose concentrations were measured using a Bio-tek FLx 800 Microplate Fluorescence Reader and an Invitrogen Amplex Red Glucose/Glucose Oxidase Assay Kit. Repeated analyses of gravimetrically prepared glucose standards yielded an uncertainty better than ±5%. Elemental concentrations were measured by Inter-Mountain Laboratories in Sheridan, WY, using a combination of ICP-OES (Varian Vista Pro CCD) and ICP-MS (Varian Ultra Mass 700). Elemental concentrations are better than ±5%. Detection limits were: Ca(1.3 μmol/L), Mg(2.1 μmol/L), P(0.2 μmol/L), Fe(0.9 μmol/L), Na(2.0 μmol/L), Si(3.6 μmol/L), Sr(0.06 μmol/L), and Ba(0.04 μmol/L). Saturation indices for major minerals were calculated using Geochemist's Workbench.

3. RESULTS AND DISCUSSION

3.1. Basalt mineralogy and geochemistry

Table 1 shows the chemical composition of the bulk basalt and its major minerals. By volume, the CRFB used in

Table 1
Chemical composition of the bulk basalt and its major components and the volume proportions of its major components[a]

	(vol %)	SiO_2 (wt%)	Al_2O_3 (wt%)	Fe_2O_3(T) (wt%)	FeO (wt%)	MnO (wt%)	MgO (wt%)	CaO (wt%)	Na_2O (wt%)	K_2O (wt%)	TiO_2 (wt%)	P_2O_5 (wt%)	LOI (wt%)	Total (wt%)
Basalt		49.18	13.54	15.45	n.m.	0.22	4.87	8.48	2.75	1.45	2.99	0.69	0.35	99.99
Pyroxene	29.3	49.87	1.23	n.m.	20.84	0.47	13.16	12.23	0.17	0.02	0.83	—	—	98.82
Glass	22.4	76.11	12.37	n.m.	0.88	0.02	0.01	0.48	1.12	5.48	0.53	—	—	97.01
Feldspar	40.8	57.02	27.25	n.m.	0.85	—	—	8.53	6.05	0.81	—	—	—	100.51
Apatite[b]	1.2							48.4				40.9		99.3
Ilmenite[b]	3.2				46.2						53.8			100

[a] n.m. denotes not measured and — denotes below detection limit.
[b] Theoretical stoichiometry of chlorapatite $Ca_5(PO_4)_3Cl$ and ilmenite $FeTiO_3$.

this study contains 40.8% feldspar (95% plagioclase and 5% orthoclase), 29.3% clinopyroxene ($Mg_{0.76}Fe_{0.68}Ca_{0.51}Al_{0.06}Si_{1.94}O_6$), 22.4% glass, 3.2% illmenite, and 1.2% apatite (Table 1). No olivine was detected. In brief, Ca mainly occurs in feldspar and pyroxene, Mg mainly occurs in pyroxene, and Fe mainly occurs in pyroxene and ilmenite. Glass is relatively devoid of elements other than Si, Al, and K. The only source of P is apatite, which occurs as needles within feldspar and glass. We were unable to directly determine the composition of apatite with the microprobe due to the small grain size of the needles (~2 μm). According to Roberts et al. (2004), apatite in CRFB occurs as chlorapatite ($Ca_5(PO_4)_3Cl$).

3.2. Glucose consumption, bacterial growth, and pH trends

Table 2 shows the pH, glucose concentrations, and cell densities measured in the growth media and the experimental reactors. Hereafter, we assume that the initial compositions of the reactor solutions (time = 0 days) were equivalent to those of the respective growth media. Immediately after inoculation, reactors B1, B2, B3, and B4 had initial cell densities of $\sim10^4$–10^5 CFU/mL. Within 4–7 days, glucose concentrations decreased to zero (Table 2, Fig. 1a). Simultaneously, cell densities increased to a maximum of $\sim10^8$ CFU/mL (Table 2, Fig. 1b). Between days 4 or 7 and 36, cell densities remained constant at $\sim10^8$ CFU/mL.

We interpret the glucose and cell density trends to reflect simple exponential bacterial growth followed by a prolonged stationary phase most likely sustained by the internal recycling of organic matter and nutrients (Finkel, 2006). We infer that no foreign microorganisms contaminated the reactors. Firstly, each plate counting experiment yielded morphologically identical cell colonies. Secondly, according to observations by confocal scanning laser microscopy, the size (~1 μm length) and shape of the bacteria (rod) remained consistent throughout the entire experimental period (Wu et al., 2006). Neither glucose consumption nor viable cells were observed in the five control reactors (Table 2, Fig. 1a). Although we are unable to explain the glucose data for C3, it is unlikely that the pattern resulted from bacterial metabolism, since the reactor did not contain viable cells or display any other characteristics of microbial activities (e.g., pH changes).

In the case of the *P-limited* experiments, the most plausible explanation for prolific cell growth is that *B. fungorum* utilized apatite as a P source for biomass synthesis (e.g., Welch et al., 2002; Rogers and Bennett, 2004). Results obtained from reactors B5 (bacteria + *P-limited medium* − basalt) and B6 (bacteria + *P-bearing medium with* KH_2PO_4 − basalt) support this assertion. The cell density in B5 increased one order of magnitude to $\sim10^6$ CFU/mL after 1 day, remained constant between days 2 and 7, and then decreased to $\sim10^5$ CFU/mL by day 36 (Fig. 1b). By comparison, the cell density in B6 increased 3 orders of magnitude to $\sim10^8$ CFU/mL by day 2 and remained constant until day 36 (Fig. 1b). In B5, *B. fungorum* likely adapted to the P-limited environment by assimilating P from complex sources, such as inert cells or extracellular polysaccharides, consequently utilizing less P on a per cell

Table 2
General characteristics of reactor solutions[a]

Reactor ID	Time (days)	pH	Log (cell density) (CFU[b]/mL)	Glucose (μmol/L)	Ba (μmol/L)	Ca (μmol/L)	Fe (μmol/L)	K (μmol/L)	Mg (μmol/L)	Na (μmol/L)	P (μmol/L)	Si (μmol/L)	Sr (μmol/L)
P-limited medium		6.50	—	1274	—	—	—	6	—	7	—	—	—
P-limited medium (low pH)		4.34	—	n.m.	—	3.8	—	15	4	14	—	—	0.08
P-bearing medium (NaH_2PO_4)		6.88	—	1109	—	—	—	12	—	2809	2755	4	—
P-bearing medium (KH_2PO_4)		6.84	—	1395	—	—	—	206	3	—	243	—	—
B1	1	6.28	0.30	1385	—	10.8	—	18	—	20	—	11	—
	4	4.01	7.68	552	—	46.8	2.2	16	15	15	—	28	0.09
	7	4.54	8.49	3	0.07	89.8	10.8	24	35	19	—	57	0.18
	10	4.82	8.26	3	0.07	102	14.5	21	43	20	—	78	0.22
	13	5.05	8.20	3	0.11	129	19.2	23	73	20	—	100	0.27
	16	4.90	8.34	3	0.10	123	13.1	16	60	17	—	103	0.25
	23	5.10	8.32	3	0.11	135	15.4	21	72	21	—	132	0.27
	30	5.24	8.48	2	0.11	138	12.4	24	77	21	—	153	0.30
	36	5.10	8.32	2	0.12	146	10.0	37	86	25	—	171	0.31
B2	1	5.39	6.90	1309	—	11.5	—	16	—	12	—	11	—
	4	4.38	8.04	2	0.05	79.3	10.9	16	29	16	—	46	0.16
	7	4.67	7.84	3	0.07	94.5	11.3	21	38	18	—	68	0.19
	10	4.80	8.28	3	0.07	102	14.0	21	42	20	—	82	0.21
	13	4.90	8.26	3	0.10	136	17.7	19	69	17	—	103	0.27
	16	4.99	8.30	3	0.10	133	13.8	17	69	19	—	107	0.25
	23	5.05	8.30	2	0.12	163	14.2	22	85	21	—	149	0.33
	30	5.17	8.20	2	0.10	148	9.9	25	77	20	—	153	0.29
	36	5.20	8.18	1	0.10	158	7.7	22	84	22	—	167	0.31
B3	1	6.60	7.11	1166	—	13.3	—	24	—	2665	2642	14	—
	4	6.04	7.65	146	—	26.0	—	19	6	2678	2619	28	—
	7	6.28	7.23	0	—	33.0	—	23	15	2730	2697	46	—
	10	6.52	7.60	0	—	35.8	—	23	17	2765	2710	57	—
	13	6.64	7.76	0	—	28.5	—	19	14	3009	2739	57	0.11
	16	6.66	7.72	0	—	33.3	—	21	18	3265	2755	75	0.11
	23	6.56	7.57	0	—	40.3	—	35	27	3704	3452	117	0.15
	30	6.72	7.51	0	—	45.0	—	35	28	3470	3055	121	0.08
	36	6.74	7.38	0	—	49.5	—	41	31	3530	3168	139	0.08
B4	1	4.15	8.08	836	—	11.8	—	237	—	121	201	25	—
	4	5.42	8.48	0	0.04	67.8	4.1	238	19	127	168	60	0.10
	7	5.78	8.49	0	—	84.0	1.3	251	23	131	167	71	0.11
	10	5.98	8.60	0	—	88.5	—	236	24	140	167	82	0.11
	13	6.15	8.51	2	—	89.3	—	229	25	132	167	89	0.10
	16	6.34	8.52	4	—	89.3	—	175	26	105	171	107	0.18
	23	6.50	8.49	0	—	107	—	204	31	133	198	142	0.21
	30	6.66	8.48	0	—	105	—	219	32	107	182	142	0.17
	36	6.67	8.38	0	—	111	—	212	36	113	195	153	0.17

C1	1	6.73	—	1283	—	2.0	—	30	2	132	—	18	—
	4	6.94	—	1353	—	8.8	—	30	3	133	—	28	—
	7	7.12	—	1171	—	17.3	—	40	5	136	—	39	—
	10	7.19	—	1395	—	21.5	—	94	7	144	—	43	—
	13	7.08	—	1255	—	31.8	—	30	10	142	—	50	—
	16	7.09	—	1339	—	34.0	—	30	11	146	—	53	—
	23	7.02	—	1283	—	38.0	—	18	13	114	—	68	0.11
	30	7.21	—	1297	—	43.5	—	21	12	117	—	82	0.13
	36	7.22	—	1353	—	48.3	—	35	15	117	5	89	0.10
C2	1	6.58	—	1465	—	2.8	—	38	—	131	—	14	—
	4	6.84	—	1437	—	8.0	—	75	4	143	—	25	—
	7	6.92	—	1479	—	11.0	—	27	5	135	—	36	—
	10	6.98	—	1367	—	15.8	—	31	7	140	—	43	—
	13	6.94	—	1423	—	17.0	—	30	7	138	—	46	—
	16	6.91	—	1339	—	17.8	—	28	9	140	—	53	—
	23	6.82	—	1395	—	19.3	—	20	8	120	—	71	0.14
	30	7.00	—	1437	—	27.0	—	28	13	116	—	82	0.11
	36	7.16	—	1409	—	29.0	—	198	14	134	—	93	0.07
C3	1	6.76	—	1003	—	13.0	—	40	5	2596	2735	25	—
	4	6.84	—	933	—	26.8	—	51	10	2600	2752	36	—
	7	6.87	—	933	—	24.8	—	50	10	2643	2729	46	—
	10	6.87	—	947	—	31.5	—	101	14	2665	2797	53	—
	13	6.80	—	989	—	31.5	—	43	12	2696	2806	64	—
	16	6.81	—	1269	—	40.5	—	39	16	2722	2813	71	0.06
	23	6.80	—	1003	—	39.3	—	36	18	3413	2858	100	0.14
	30	6.87	—	947	—	47.5	—	35	24	3548	2981	114	0.15
	36	6.85	—	933	—	48.8	—	35	17	2991	3013	128	0.11
C4	1	6.88	—	1283	—	10.3	—	269	3	117	223	25	—
	4	7.17	—	1269	—	47.8	—	225	9	118	223	36	—
	7	7.22	—	1269	—	61.5	—	233	11	121	227	43	0.07
	10	7.25	—	1269	—	68.8	—	245	11	132	219	50	0.07
	13	7.25	—	1339	—	75.5	—	232	14	128	227	53	0.08
	16	7.27	—	1213	—	73.3	—	163	9	97	206	64	0.15
	23	7.28	—	1339	—	89.5	—	199	16	130	252	85	0.19
	30	7.27	—	1381	—	89.8	—	197	19	97	249	89	0.11
	36	7.29	—	1339	—	99.3	—	210	23	104	255	96	0.14
	Time (h)												
C5	4	6.12	—	1276	—	8.3	—	20	4	80	—	11	—
	8	6.61	—	1325	—	17.8	—	121	6	97	3	14	—
	12	6.91	—	1268	—	24.3	—	46	6	87	—	18	—
	24	7.14	—	1219	—	51.8	—	50	10	95	—	21	0.08
	28	7.22	—	1284	—	60.0	—	23	9	97	—	25	0.08
	32	7.32	—	1382	—	71.0	—	125	12	93	7	25	0.10
	36	7.33	—	1268	—	80.5	—	33	13	91	—	25	0.10
	48	7.33	—	1325	—	96.8	—	22	14	85	—	28	0.11

[a] Raw elemental concentrations.
[b] CFU, Colony Forming Units.

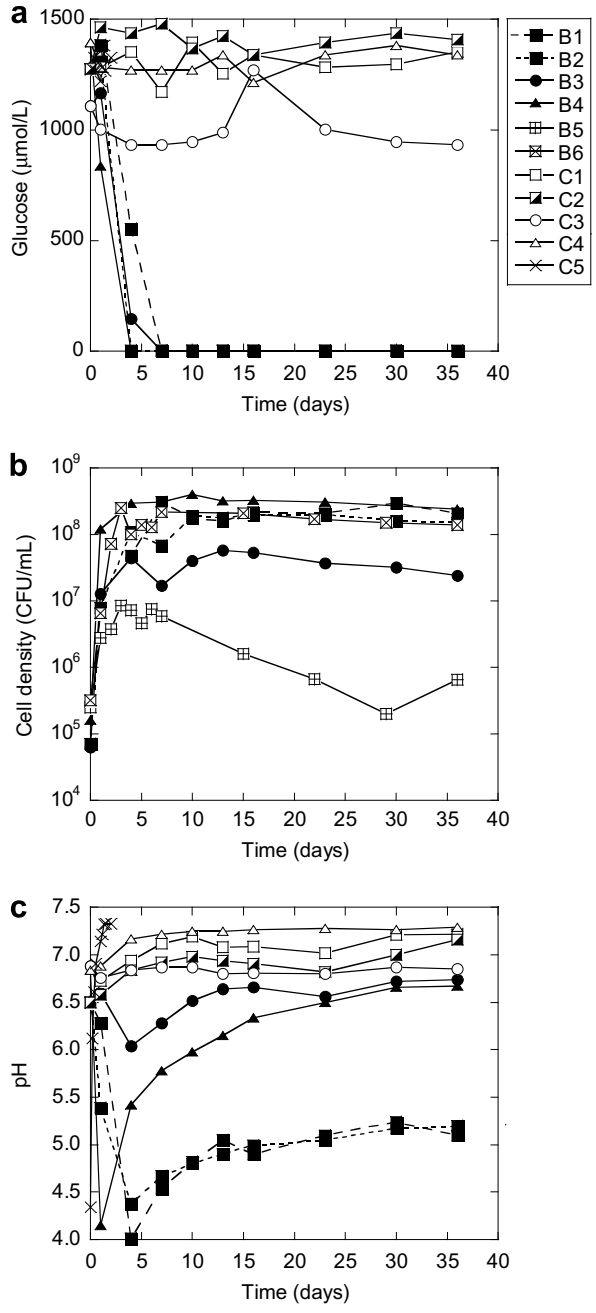

Fig. 1. Glucose concentrations (a), cell density (b), and pH (c) versus time for all experimental reactors (see Section 2.5). Data for reactors B5 and B6 only appear in (b).

basis (Allison and Vitousek, 2005). However, this process reached a maximum and ultimately led to a net decrease in viable cells. Because the cell growth pattern observed for B6 is virtually identical to the patterns observed for the other biotic reactors containing basalt, in particular B1 and B2, we infer that *B. fungorum* utilized apatite-bound P for biomass synthesis.

Coincident with the period of exponential cell growth and glucose depletion, the pH in all biotic reactors rapidly decreased from an initial value of 6.68. The pH in reactors B1 and B2 decreased to 4.20 by day 4. The pH in reactors B3 decreased to 6.04 by day 4, and the pH in B4 decreased to 4.15 by day 1. Following the period of cell growth and glucose utilization, pH values gradually increased. By day 36, the pH in reactors B1 and B2 rose to 5.15, while the pH in reactors B3 and B4 rose to 6.70. As discussed below in more detail, we attribute the initial acidification to microbial metabolism and the final pH increase to proton uptake during elemental release from basalt. The higher final pH in reactors B3 and B4 (*P-bearing media*) versus B1 and B2 (*P-limited medium*) most likely resulted from the added effect of buffering by dissolved P species (Stumm and Morgan, 1981). Reactor B3 displayed a smaller pH variation relative to B4 because B3 contained an order of magnitude more P (2755 versus 243 μmol/L).

In contrast to the biotic reactors, the pH in control reactors C1, C2, C3, and C4 generally remained near neutral, which is consistent with lack of microbial activity in these experiments. The pH slightly increased by day 1, most likely due to modest proton uptake during elemental release, and then leveled off with time. This pattern is consistent with prior work focusing on inorganic basalt dissolution (e.g., Gislason and Eugster, 1987b; Gislason et al., 1993). The one exception to the aforementioned trends is C5, which was initiated at pH 4.34 in an attempt to simulate the behavior of the biotic reactors. Unlike the biotic experiments, the pH of this experiment rapidly rose to 7.33 by day 2, thus suggesting that HCl-mediated dissolution is not an ideal analogue for microbially mediated dissolution.

3.3. Source of acidity

Here, we develop a stoichiometric equation for bacterial growth to explore factors that led to the initial pH decrease observed in the biotic reactors. In our experiments, *B. fungorum* used glucose as both an energy source (electron donor) and a carbon source for biomass synthesis. We can write the energy reaction (aerobic glucose oxidation) as:

$$C_6H_{12}O_6 + 6O_2 \rightarrow 6CO_2 + 6H_2O \quad (1)$$

and the cell synthesis equation, using NH_4^+ as a N source, as:

$$7C_6H_{12}O_6 + 8NH_4^+ + 8HCO_3^- \rightarrow 8C_5H_8O_2N + 10CO_2 + 30H_2O \quad (2)$$

where $C_5H_8O_2N$ is an assumed chemical formula for a pure culture of prokaryotic cells (Rittman and McCarty, 2000). Assuming that *B. fungorum* used 80% of the electron equivalents in glucose for energy production and the remaining 20% for cell synthesis (Rittman and McCarty, 2000), we can write the overall reaction for microbial growth as:

$$11C_6H_{12}O_6 + 24O_2 + 8NH_4^+ + 8HCO_3^- \rightarrow 8C_5H_8O_2N + 34CO_2 + 54H_2O \quad (3)$$

Given Eq. (3), one hypothesis to explain the lowered pH is that the bacteria produced carbonic acid (H_2CO_3) by sparging respired CO_2 directly into the reactor solutions. This phenomenon has been widely observed in both natural and experimental settings, even under conditions partially open to the atmosphere (Ho et al., 1987; Morel and Hering,

1993; VanBriesen and Rittman, 1999). If we make the simplifying assumption that the rate of CO_2, and hence, H_2CO_3, addition to solution is sufficiently fast relative to reactions governing CO_2 loss (e.g., diffusion, basalt dissolution etc.), we can use Eq. (3) and relations governing the dissolved carbonate system to estimate the maximum possible effect of microbial metabolism on solution pH. The initial glucose concentration in B1 and B2 was 1274 μmol/L. According to Eq. (3), the complete consumption of glucose would yield 2752 μmol/L of CO_2 ($= H_2CO_3^*$). At $T =$ 30 °C, the pK_a of $H_2CO_3^*$ is 6.33 ($K \cong [H^+][HCO_3^-]/[H_2CO_3^*]$). Thus, respired CO_2 could have lowered pH to 4.45, which is in reasonable agreement with the measured values of 4.54, 4.38, and 4.15 in B1, B2, and B4, respectively.

An alternative hypothesis is that the lowered pH resulted from production of organic acids. Previous work concerning a related microorganism (*Burkholderia solanecerum*) has shown that the partial oxidation of glucose can lower pH via the production of gluconic acid (Welch and Ullman, 1999). Gluconic acid accumulates in the medium until glucose is exhausted, at which time bacteria respire gluconate to CO_2. To quantify the effect, it is necessary to measure gluconate concentrations. Although we did not conduct such measurements, we can use data presented in Welch and Ullman (1999) to estimate the amount of gluconic acid produced in our experiments, recognizing that gluconic acid production depends on many factors, such as the nutritional, physiological, and growth conditions of various cultures. According to Welch and Ullman (1999), a maximum of ~10% of the initial glucose was released as gluconic acid at $T = 20$ °C. Given our initial glucose concentration of 1274 μmol/L, we estimate that *B. fungorum* could have produced 127 μmol/L of gluconic acid. Gluconic acid is a weak acid with a pK_a of 3.7 (Ramachandran et al., 2006). Thus, the theoretical pH of a 127 μmol/L gluconic acid solution is 4.05, which is also broadly consistent with the measured values in reactors B1, B2, and B4.

Lastly, other laboratory work has shown that bacteria as well as fungi can acidify their surrounding medium through an ionic exchange mechanism involving the uptake of NH_4^+ and the extrusion of H^+ with a 1:1 stoichiometry (Roos and Luckner, 1984; Gyaneshwar et al., 1998; Reyes et al., 1999). This reaction is especially pervasive in experimental systems such as ours, where glucose is supplied as a C source and ammonium is supplied as a N source. Although we did not measure NH_4^+ concentrations, we may use Eq. (3) to estimate the pH drop associated with the NH_4^+–H^+ exchange mechanism. According to Eq. (3), the complete consumption of 1274 μmol/L of glucose would yield 1223 μmol/L of cells. Each bacterial cell contains one mole of N, thus yielding a theoretical pH of 2.9. Although this result is considerably lower than the measured values, we nonetheless view the exchange mechanism as plausible given the approximate nature of the calculations. For example, none of our calculations consider the amount of H^+ lost by reaction with basalt, which would raise all of the aforementioned pH estimates to higher values. While additional work is required to constrain the source of acidity in our experiments, it is clear that microbial metabolism led to substantial changes in solution pH. As discussed in the following section, these changes had important consequences for the rate of elemental release from basalt compared to abiotic conditions.

3.4. Dissolved elemental concentrations

Table 2 lists the elemental concentrations measured in the growth media and the experimental reactors. Aside from Na, K, and P, all elements in the growth media were below detection limit, thus confirming that basalt supplied the remaining elements in the reactor solutions. The very high Na, K, and P concentrations in the *P-bearing media* resulted from the reagents used to construct the media (see Section 2.2). To evaluate the concentration data in more detail, we first corrected the raw results reported in Table 2 for the decrease in fluid volume and the loss of elemental mass during sampling using the equation:

$$C^*_{j,i} = \frac{C_{j,i}[V_0 - (j-1)V_s] + \sum_{h=1}^{j-1} C_{h,i} V_s}{V_0} \quad (4)$$

where $C^*_{j,i}$ is the corrected concentration of element i in the jth sample ($j = 1,2,\ldots,9$), $C_{j,i}$ is the measured concentration (Table 2), V_0 is the initial fluid volume (0.2 L), V_s is the sampling volume (0.0103 L), and the term $\sum_{h=1}^{j-1} C_{h,i} V_s$ accounts for the mass of element i extracted during sampling. By comparing initial and final fluid volumes, we estimate that ~10% of the fluid evaporated over the course of the experiments. The correction does not account for this loss because we do not know how evaporation varied with time. However, since evaporation likely affected all reactors in the same way, it is reasonable to ignore the effect because our primary goal is to make relative comparisons between the biotic and abiotic experiments.

Fig. 2 shows the corrected elemental concentrations as a function of time. In general, we observed the highest elemental concentrations in the *P-limited* reactors (B1 and B2), followed by the *P-bearing* reactors (B3 and B4) and the abiotic controls. Most elemental concentrations (Ba, Ca, Mg, Si, and Sr) increased linearly until days 7 to 10 and then either reached or began to approach apparent, near steady-state conditions. This parabolic pattern is common to batch dissolution experiments (e.g., Wollast, 1967; Luce et al., 1972; Busenberg and Clemency, 1976). We interpret the data to represent incongruent elemental release controlled by two phenomena giving rise to essentially the same elemental profiles, namely ion diffusion through a thickening leached layer and the approach to saturation with respect to secondary phases (e.g., hydrous alumino-silicates) (e.g., Wollast, 1967; Luce et al., 1972; Paces, 1973; Eick et al., 1996). We can reasonably discount the dissolution of ultrafine particles because the basalt was thoroughly cleaned prior to use (Holdren and Berner, 1979).

We evaluated mineral saturation indices using Geochemist's Workbench. All solutions were undersaturated with respect to calcite. B3 and B4 were saturated with respect to whitlockite ($Ca_3(PO_4)_2$) and hydroxyapatite (log $K_{sp} = -11.5$ at $T = 25$ °C) owing to the relatively high P concentrations in the *P-bearing* media. We evaluated the a_{Ca}/a_H^2 vs a_{Si} composition of the fluids to examine their stability

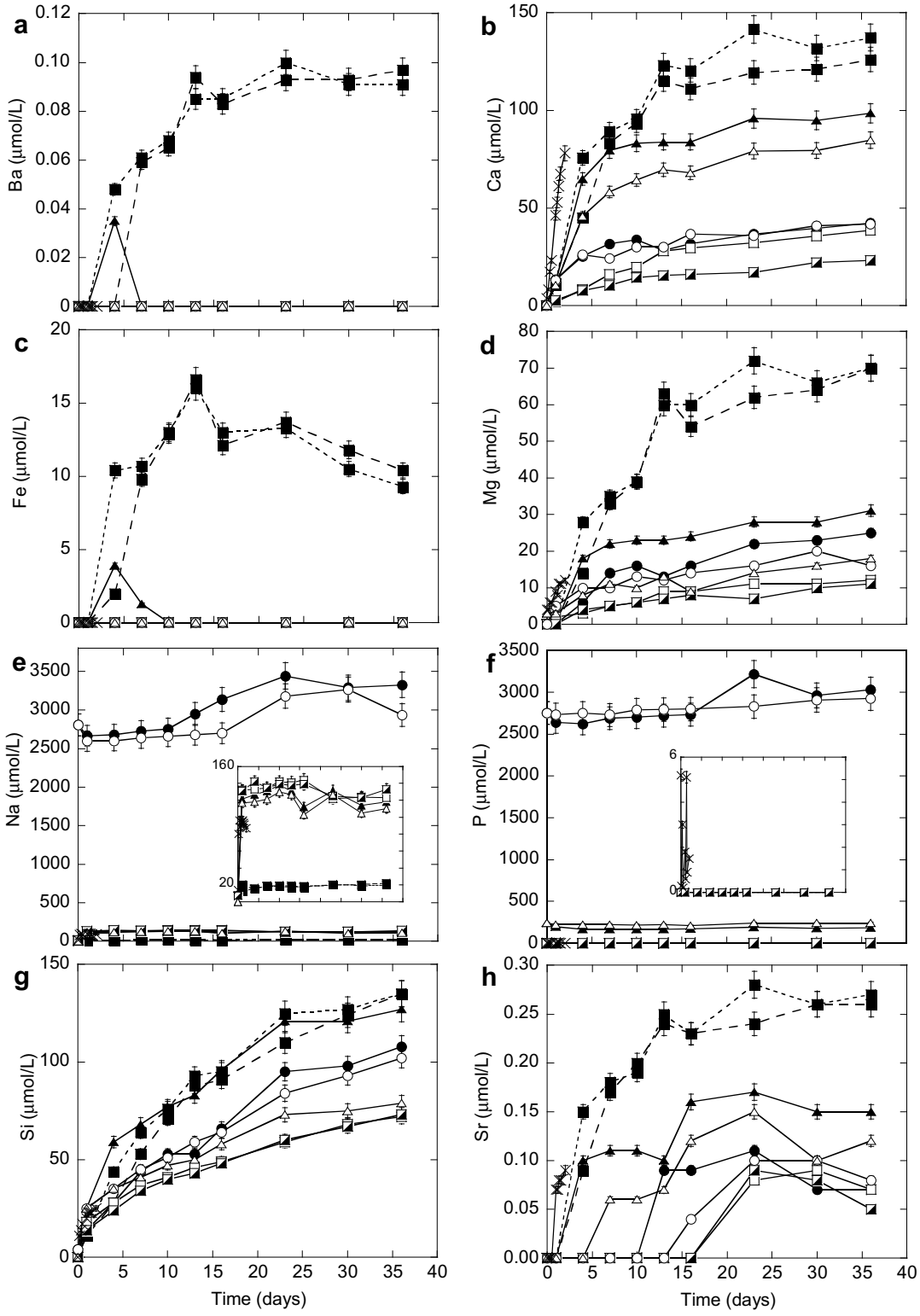

Fig. 2. Ba (a), Ca (b), Fe (c), Mg (d), Na (e), P (f), Si (g), and Sr (h) concentrations versus time for all experimental reactors. Error bars indicate 5% relative uncertainty. Symbols identical to Fig. 1.

with respect to various clay minerals (Gislason and Eugster, 1987b). The solutions were stable with respect to gibbsite and kaolinite but not smectite. Hence, it is reasonable to assume that Si (and Al, although it was not measured as part of the study) were removed from solution. It is less likely that the formation of gibbsite and kaolinite removed Ba,

Ca, Mg, and Sr because in general, these minerals do not contain appreciable concentrations of divalent cations. Nonetheless, we cannot entirely rule out the possibility that divalent cations adsorbed onto secondary mineral surfaces. Lastly, we cannot discount ion removal in the biotic reactors by organic precipitates (e.g., Ca-oxalate) (Welch et al., 2002) because we did not evaluate particle surfaces at the end of the experiments. However, because Ca concentrations in the abiotic reactors leveled off with time in a manner similar to the biotic reactors, we do not view this effect as critical in our experiments. We therefore conclude that Ba, Ca, Mg, Si, and Sr release rates decreased with time as a consequence of the kinetic limitations noted above.

Exceptions to the aforementioned behavior include Fe, P, K, and Na. The Fe concentrations in B1 and B2 increased linearly until day 13 and then decreased. This trend may reflect an initial enhancement of Fe release due to the presence of microbially produced chelators followed by Fe removal by either biological uptake or the formation of secondary Fe phases (Liermann et al., 2000). P concentrations in B1, B2, C1, and C2 were below the detection limit of the method. The high P concentrations in the remaining reactors reflect the composition of the *P-bearing media*. Fig. 2 does not include K because no trends were observed. In general, basalt is not a significant reservoir of K. B3 and C3 had high Na concentrations due to the addition of NaH_2PO_4. However, in contrast to other base cations, C1, C2, and C4 had much higher levels of Na than B1 and B2. The levels were even higher than that observed in C5, which had an initial pH of 4.3. We attribute this pattern to the incomplete removal of bleach during the particle sterilization procedure. Hereafter, we exclude K and Na from further consideration.

3.5. Elemental release rates

In this section, we evaluate the kinetics of Ba, Ca, Mg, Fe, Si, and Sr release using two rate laws, a linear rate law and a bulk-effective rate law. The linear rate law (zeroth order kinetics) yields a straightforward result that describes elemental release under far-from-equilibrium conditions (Brantley, 2003). The linear rate law is one of the most widely utilized rate laws. Thus, we report linear release rates so that direct comparisons can be made to other studies.

We use the bulk-effective rate law to describe the gross chemistry of the reactor fluids throughout the entire experimental period. The bulk-effective rate law provides a more complete interpretation of the data relative to the linear rate law, in that it accounts for the effect of changing fluid chemistry on elemental release (Wollast, 1967). This rate law, or some variation thereof, is most commonly utilized to quantify the dissolution of individual minerals, but a few studies have applied the rate law to mixed phase systems (Paces, 1973; Lerman, 1979). More sophisticated rate laws have been developed for describing the dissolution of multioxide silicates (Oelkers, 2001), but their implementation requires key information not available for the present study, including equilibrium constants for metal/proton exchange reactions, the stoichiometry of the precursor complex, and dissolution rate constants. Although the bulk-effective rate law is less complex, it is sufficient for making relative comparisons between the biotic and abiotic reactors.

The linear rate law is given by the equation:

$$R_i^{\mathrm{l}} = \frac{\mathrm{d}C_i^*}{\mathrm{d}t}\frac{V_0}{Am}, \tag{5}$$

where R_i^l is the linear release rate of element i (mol/m^2/s), $\mathrm{d}C_i^*/\mathrm{d}t$ is the slope of the line describing C_i^* versus time in Fig. 2 over the interval of 0 to 7 or 10 days, V_0 is the initial fluid volume (0.2 L), A is the BET-N_2 surface area (5.57 m^2/g), and m is the mass of basalt particles (2 g).

The bulk-effective rate law is given by the equation:

$$R_i^{\mathrm{be}} = k_i(C_i^{\mathrm{eq}} - C_i^*)\frac{V_0}{Am}, \tag{6}$$

where R_i^{be} is the release rate of element i (mol/m^2/s), k_i is a first-order rate constant for the release of element i, C_i^{eq} is the equilibrium concentration of element i (mol/L), C_i^* is the corrected concentration of element i (mol/L), and the remainder of the parameters are defined above. C_i^{eq} is estimated by extrapolation to infinite time (Garrels et al., 1960; Plummer and Mackenzie, 1974). For the elements that reached near steady state conditions (e.g., Ca and Mg), C_i^{eq} approximately equals the maximum concentration in the reactor solutions. Eq. (6) does not account for ion removal by secondary mineral formation.

The rate constant, k_i, is obtained by noting that

$$\frac{\mathrm{d}C_i^*}{\mathrm{d}t} = k_i(C_i^{\mathrm{eq}} - C_i^*), \tag{7}$$

which when integrated yields

$$\ln(C_i^{\mathrm{eq}} - C_i^*) = \ln(C_i^{\mathrm{eq}} - C_i^0) - k_i t, \tag{8}$$

where C_i^0 is the initial concentration of element i in the reactor at time zero (the growth medium reported in Table 2). Plotting $\ln(C_i^{\mathrm{eq}} - C_i^*)$ versus $-t$ yields a line with a slope equal to k_i.

Inspection of Eq. (6) shows that the release rate, R_i^{be}, varies with concentration (or time). R_i^{be} is maximum when $C_i^* = C_i^0$ and zero when $C_i^* = C_i^{\mathrm{eq}}$. To aid comparisons between the various reactors, it is convenient to calculate the average release rate of element i ($\bar{R}_i^{\mathrm{be}}$) over the course of the entire experiment:

$$\bar{R}_i^{\mathrm{be}} = \left[\frac{C_i^{\mathrm{eq}}(1 - \mathrm{e}^{-k_i t_{\mathrm{f}}}) - C_0}{t_{\mathrm{f}}}\right]\frac{V_0}{Am}, \tag{9}$$

where t_{f} is the final sampling time (36 days).

Table 3 shows results for the linear rate law and the bulk-effective rate law, including k_i, $\bar{R}_i^{\mathrm{be}}$, and the maximum value of R_i^{be} at $t = 0$ day. When fit to the data, both rate laws generally yield R^2 values greater than 0.90, although a few are between 0.70 and 0.80. The most notable exceptions pertain to Sr and Fe. In some cases, there were too few data for Sr to obtain reliable fits. The bulk-effective rate law is not appropriate for Fe because Fe concentrations decreased after 13 days. Overall, for Ca, Mg, and Sr, the linear rate law gives a slightly better fit than the bulk-effective rate law and vice versa for Si.

Consistent with the equations presented above, release rates calculated with the linear rate law are ~2- to 4-fold

Table 3
Linear elemental release rates (R_i^l) calculated from linear rate law and rate constants (k_i), average elemental release rates ($\bar{R}_i^{be}$) and maximum elemental release rates (R_i^{be}) calculated from the bulk-effective rate law

Reactor ID	Ba	Ca	Fe	Mg	Si	Sr
R_i^l (10^{-12} mol/m^2/s)						
B1	0.0016	2.47	0.28	1.00	1.51	0.0050
B2	0.0020	2.84	0.37	1.17	1.92	0.0057
B3	—	0.87	—	0.43	1.13	—
B4	—	2.49	—	0.72	1.95	0.0037
C1	—	0.47	—	0.13	0.99	—
C2	—	0.30	—	0.15	0.91	—
C3	—	0.67	—	0.27	1.06	—
C4	—	1.79	—	0.31	1.05	0.0017
C5	—	8.36	—	0.82	6.87	0.012
k_i (1/day)						
B1	0.127	0.174	0.034	0.09	0.08	0.136
B2	0.068	0.091	0.022	0.10	0.10	0.082
B3	—	0.076	—	0.09	0.08	0.036
B4	—	0.177	—	0.10	0.10	0.064
C1	—	0.087	—	0.08	0.08	—
C2	—	0.083	—	0.07	0.08	—
C3	—	0.110	—	0.04	0.07	—
C4	—	0.093	—	0.06	0.10	0.042
$\bar{R}_i^{be}$ (10^{-12} mol/m^2/s)						
B1	0.0009	0.98	0.07	0.54	1.11	0.0021
B2	0.0006	0.96	0.05	0.53	1.15	0.0018
B3	—	0.34	—	0.24	1.03	—
B4	—	0.66	—	0.19	1.07	0.0009
C1	—	0.31	—	0.09	0.57	—
C2	—	0.16	—	0.07	0.60	—
C3	—	0.31	—	0.08	0.82	—
C4	—	0.52	—	0.09	0.62	0.0009
Maximum R_i^{be} (10^{-12} mol/m^2/s)						
B1	0.0040	6.14	0.12	1.85	3.42	0.0102
B2	0.0017	3.29	0.07	1.90	4.20	0.0055
B3	—	0.99	—	0.78	3.15	—
B4	—	4.21	—	0.68	4.12	0.0024
C1	—	1.01	—	0.26	1.78	—
C2	—	0.49	—	0.20	1.77	—
C3	—	1.26	—	0.15	2.35	—
C4	—	1.82	—	0.22	2.53	0.0017

higher than the average release rates calculated with the bulk-effective rate law. Nonetheless, both rate laws show that B1 and B2 experienced higher release rates relative to C1 and C2 for all elements. Ca release rates in B1 and B2 were ~3- to 9-fold higher relative to C1 and C2. Similarly, for Mg and Si, the relative differences were ~6- to 9-fold and 2-fold, respectively. The Sr release rates were elevated several orders of magnitude because Sr was generally below detection limit in C1 and C2.

Among the control reactors, the Ca release rates in C1 were ~2-fold higher relative to C2, the control reactor that contained inert cells. The Mg and Si release rates were comparable between C1 and C2. We conclude from these latter results that the chemical properties of cell surfaces are less critical than active metabolism in terms of influencing elemental release from basalt. Reactor C5, which was adjusted to pH 4 with HCl, experienced the highest Ca, Mg, Si, and Sr release rates compared to all other reactors. Surprisingly however, B1 and B2 yielded orders of magnitude greater Fe and Ba release rates relative to C5. The high Fe release rate may have resulted from the presence of microbially produced chelators (Liermann et al., 2000; Kraemer, 2004; Aouad et al., 2006). A similar mechanism may explain the Ba release rates. This could have implications for understanding dissolved Ba fluxes from basaltic watershed (Das and Krishnaswami, 2006). However, more work is required to understand microbial controls on Ba geochemistry. Overall, comparisons between B1, B2, and C5 demonstrate that HCl mediated dissolution is not an appropriate analogue for microbially mediated dissolution.

The linear Ca, Mg, Na, and Si release rates reported here are either equal to or ~2-fold lower than those for crystalline basalt (Gislason and Eugster, 1987b), with the exception of C5. However, these rates were determined under basic conditions (pH 9), where dissolution proceeds more rapidly relative to the pH conditions examined in this study (Oelkers and Gislason, 2001; Brantley, 2003; Gislason and Oelkers, 2003). Likewise, the Ca and Mg release rates reported here are ~2 orders of magnitude lower than average rates compiled by Wolff-Boenisch et al. (2006). However, these rates largely correspond to dissolution by strong mineral acid solutions at pH 4, where dissolution is also expected to be rapid. Indeed, the rates reported by Wolff-Boenisch et al. (2006) are generally consistent with those determined for reactor C5, which clearly followed a different reaction path relative to the biotic reactors. In terms of biologically mediated elemental release, the Mg, Ca, and Si release rates reported here are up to ~2 orders of magnitude higher than plant-induced release rates at pH 6–7 (Hinsinger et al., 2001).

It is possible that discrepancies between biotic and abiotic release rates may in part result from the presence of organic molecules (such as extracellular polysaccharides) in biotic experiments that bind to mineral surfaces and effectively shield reactive surface sites from dissolution reactions (Sverdrup, 1990; White, 1995; Ullman et al., 1996; Welch et al., 1999; Benzerara et al., 2004, 2005). The internal comparisons made in this study demonstrate that microbial activities accelerate elemental release, but it is evident that generalizing findings among various studies is problematic due to differences in experimental conditions. As well, compared to the number of studies examining inorganic weathering phenomena, relatively few investigations have examined the release of base cations from silicate minerals in the presence of actively metabolizing bacteria. This information is required to better understand the role of bioweathering phenomena in key elemental cycles.

In either case, plotting $\bar{R}_i^{be}$ versus average pH provides strong evidence that the elemental release rates were pH dependent (Fig. 3). Consistent with prior studies focusing on the dissolution of basalt and other geologic materials, Fig. 3 shows that the highest elemental release rates occurred at low pH, while the lowest rates occurred at near-neutral pH (Blum and Stillings, 1995; Brantley, 2003; Gislason and Oelkers, 2003). We infer that ligand-promoted dissolution was less important because the *P-limited* and *P-bearing* reactors experienced nearly identical rates of

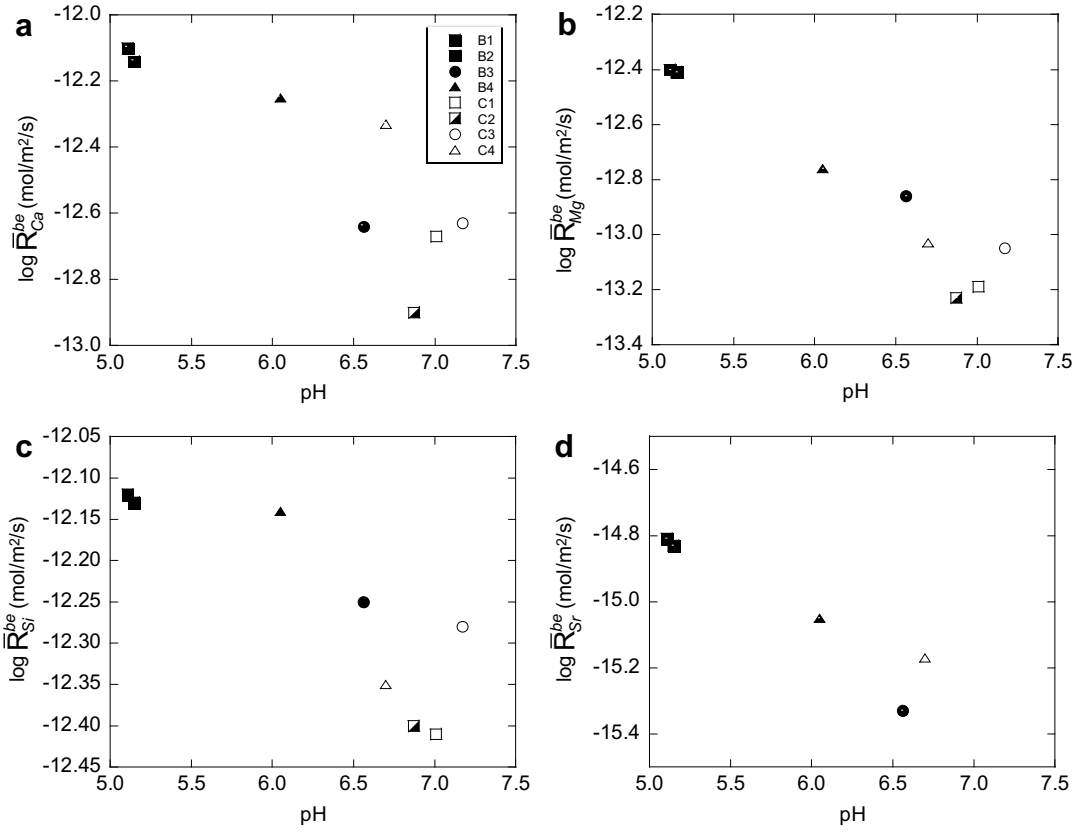

Fig. 3. Log $\bar{R}^{be}_{Ca}$ (a), $\bar{R}^{be}_{Mg}$ (b), $\bar{R}^{be}_{Si}$ (c), and $\bar{R}^{be}_{Sr}$ (d) versus average pH for all experimental reactors. $\bar{R}^{be}_{i}$ is the average bulk-effective release rate of element i calculated according to Eq. (9).

microbial growth, but the *P-bearing* reactors displayed overall lower dissolution rates at near-neutral pH, where presumably, the effect of ligand-promoted dissolution would be most evident (Vandevivere et al., 1994; Welch and Ullman, 1999). This finding does not negate the importance of ligand-promoted dissolution. Rather, it highlights the diverse range of interactions that can occur between microorganisms and geologic materials.

3.6. Elemental uptake by bacteria

Table 4 reports intracellular elemental concentrations for bacteria collected from reactors B1, B2, and B3 on day 36. We determined these values by normalizing the measured concentrations of the digested biomass to the total number of bacterial cells remaining in the reactors at the termination of the experiments [i.e., final fluid volume multiplied by the final cell density corrected according to Eq. (4)]. The intracellular elemental concentrations reported in Table 4 are likely maximum estimates because we probably digested both live and dead biomass but the cell density refers only to viable planktonic cells. As well, it is possible that the 0.2 μm filter did not capture mineral particles encrusting cell walls and/or colloidal phases mixed with bacteria.

To investigate if elemental uptake by bacteria was significant with respect to solute concentrations in the reactor fluids, we multiplied the data in Table 4 by the cell densities in Table 2, corrected according to Eq. (4). Note that while the per cell elemental concentrations reported in Table 4 could be maximum estimates, the calculation described here could produce underestimates because it does not account for cells attached to basalt particles. The calculation shows that the uptake of Ca, Fe, and Mg by bacteria was small to moderate compared to the fluid concentrations, ~0–1% for Ca, 2–7% for Fe, 0–11% for K, and 3–9% for Mg. However, P uptake was significant, especially for reactors B1 and B2, where P in the fluid phase was below detection limit (Table

Table 4
Chemical composition of planktonic cells

Reactor ID	Ba (10^{-10} μmol/cell)	Ca (10^{-10} μmol/cell)	Fe (10^{-10} μmol/cell)	K (10^{-10} μmol/cell)	Mg (10^{-10} μmol/cell)	Na (10^{-10} μmol/cell)	P (10^{-10} μmol/cell)	Sr (10^{-10} μmol/cell)
B1	—	0.01	0.02	0.07	0.10	—	0.58	—
B2	—	0.06	0.04	0.11	0.14	—	0.75	—

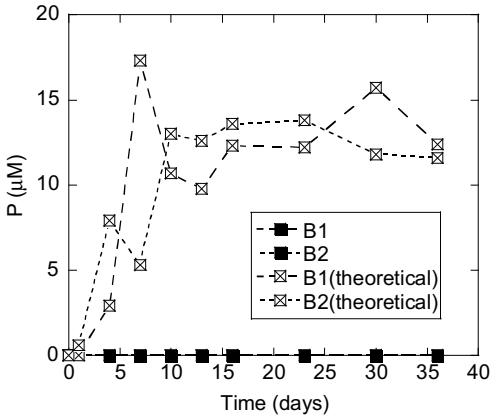

Fig. 4. Theoretical P concentrations versus time in reactors B1 and B2. See Section 3.6 for an explanation of the calculation.

2). As shown in Fig. 4, bacterial P reached levels between ~10 and 20 μmol/L with respect to the fluid. We therefore conclude that *B. fungorum* quantitatively scavenged all of the P released from apatite dissolution. However, we are unable to resolve whether *B. fungorum* directly dissolved apatite to acquire P or whether dissolution occurred as a consequence of pH lowering during growth, which in turn, stimulated additional dissolution and further growth. In either case, based on these observations, we estimate that apatite dissolution provided ~16% of the dissolved Ca in B1 and B2 and that some combination of feldspar and pyroxene dissolution provided the remainder.

Using the data in Fig. 4 and the two rate laws given above, we can calculate P release rates. According to the linear rate law, the P release rates in B1 and B2 were 0.23 and 0.24×10^{-12} mol/m^2/s, respectively. According to the bulk-effective rate law, the P release rates were 0.084 and 0.065×10^{-12} mol/m^2/s, respectively. The linear P release rates reported here are ~2–3 orders of magnitude lower than those reported elsewhere. For example, Welch et al. (2002), who used batch reactors to investigate microbially mediated apatite dissolution at pH 4–5.2 and $T = 22$ °C, reported values of 2×10^{-9}–2×10^{-10} mol/m^2/s. Köhler et al. (2005) and Guidry and Mackenzie (2003), both of whom used flow-through reactors to study fluorapatite dissolution, reported values of 0.31 and 2.4×10^{-10} mol/m^2/s at pH 6.5, respectively. This apparent discrepancy can be attributed to several factors, the most important of which is that we investigated elemental release from whole-rock samples, whereas the aforementioned studies focused on single mineral specimens. The whole-rock surface area measured for the basalt may not accurately represent the surface area of the apatite that comprises the basalt. Other possible explanations are that we underestimated the amount of P released, used different fluid-rock ratios relative to the other studies, and/or allowed the pH of our experiments to drift. Nonetheless, the general comparison between the biological and fluid phases provides reasonable evidence that the *B. fungorum* accelerated the rate of apatite dissolution relative to the abiotic control experiments.

4. CONCLUSIONS AND IMPLICATIONS

This study used batch reactors to examine how actively metabolizing bacteria (*B. fungorum*) influence elemental release from Columbia River Flood Basalt at $T = 28$ °C when utilizing glucose as a C source, ammonium as a N source, and trace apatite in the basalt as a P source. Microbial activity substantially elevated the release of Ca, Mg, Si, and Sr relative to inorganic conditions. Bacterial metabolism also accelerated the release of apatite bound P, but the liberated P was quantitatively scavenged during cell synthesis. We attribute the accelerated elemental release to pH lowering during biomass production.

While additional work is required to characterize microbial interactions with basalt and other geologic materials in both laboratory and field settings, the results of our study provide evidence that bacterial activity could have important implications for several phenomena involving continental weathering. For example, according to the experimental data presented herein, when microorganisms utilize basalt as a P source for cell synthesis, they greatly accelerate the release of dissolved Sr. Microbe–basalt interactions could therefore represent a previously overlooked mechanism linking the emplacement and weathering of basaltic provinces to the evolution of seawater $^{87}Sr/^{86}Sr$ ratios (e.g., Taylor and Lasaga, 1999; Dessert et al., 2001; Das et al., 2006). In addition to influencing the Sr isotope budget of seawater, basalt weathering is also crucial for the long-term global C cycle (e.g., Dessert et al., 2003; Dupré et al., 2003). Although the emplacement of basaltic provinces releases large quantities of CO_2 into the atmosphere, both theoretical and field studies have demonstrated that the weathering of Ca–Mg silicate minerals in basalt results in a net drawdown of CO_2 over geologic timescales (e.g., Taylor and Lasaga, 1999; Dessert et al., 2003). For every mole of Ca and Mg released by the dissolution of basaltic silicate minerals, one mole of CO_2 is removed from the atmosphere. This relationship is generally independent of the dissolving acid, in that weathering by either carbonic acid or organic acids can lead to the consumption of atmospheric CO_2 (Berner and Berner, 1996). Our study has shown that through the relatively simple mechanism of pH lowering, bacterial metabolism enhances the release of silicate-derived Ca and Mg to solution. This suggests that microbe–basalt interactions could play a role in the geochemical and climatic evolution of Earth.

ACKNOWLEDGMENTS

The authors thank Jeremy Rentz for his input and help in the lab. We also thank Fred Mackenzie and Abraham Lerman for insightful discussions. Thoughtful and highly detailed comments from Domenik Wolff-Boenisch, two anonymous reviewers, and Associate Editor Eric Oelkers greatly improved this manuscript.

REFERENCES

Allison S. D., and Vitousek P. M. (2005) Responses of extracellular enzymes to simple and complex nutrient inputs. *Soil Biol. Biochem.* **37**, 937–944.

Aouad G., Crovisier J.-L., Geoffroy V. A., Meyer J.-M., and Stille P. (2006) Microbially mediated glass dissolution and sorption of metals by *Pseudomonas aeruginosa* cells and biofilm. *J. Hazard. Mater.* **B136**, 889–895.

Babu-Khan S., Yeo T. C., Martin W. L., Duron M. R., Rogers R. D., and Goldstein A. H. (1995) Cloning of a mineral phosphate-solubilizing gene from *Pseudomonas cepacia*. *Appl. Environ. Microbiol.* **61**(3), 972–978.

Bach W., Edwards K. J., Hayes J. M., Huber J. A., Sievert S. M., and Sogin M. L. (2006) Energy in the dark: fuel for life in the deep ocean and beyond. *Eos Trans. Am. Geophys. Union* **87**(7), 73, 78.

Barker W. W., Welch S. A., Chu S., and Banfield J. F. (1998) Experimental observations of the effects of bacteria on aluminosilicate weathering. *Am. Mineral.* **83**(11–12, Part 2), 1551–1563.

Bennett P. C., Rogers J. R., Choi W. J., and Hiebert F. K. (2001) Silicates, silicate weathering, and microbial ecology. *Geomicrobiol. J.* **18**(1), 3–19.

Benzerara K., Barakat M., Menguy N., Guyot F., Luca G. D., Audrain C., and Heulin T. (2004) Experimental colonization and alteration of orthopyroxene by the pleomorphic bacteria *Ramlibacter tataouinensis*. *Geomicrobiol. J.* **21**, 341–349.

Benzerara K., Menguy N., Guyot F., Vanni C., and Gillet P. (2005) TEM study of a silicate-carbonate-microbe interface prepared by focused ion beam milling. *Geochim. Cosmochim. Acta* **69**(6), 1413–1422.

Berner E. K., and Berner R. A. (1996) *Global environment; water, air, and geochemical cycles*. Prentice Hall.

Berner R. A., and Kothavala Z. (2001) GEOCARB III: a revised model of atmospheric CO2 over Phanerozoic time. *Am. J. Sci.* **301**(2), 182–204.

Blum A. E., and Stillings L. L. (1995) Feldspar dissolution kinetics. In *Reviews in Mineralogy* (eds. A. F. White and S. L. Brantley, vol. 31.). Mineralogical Society of America, pp. 291–351.

Bluth G. J. S., and Kump L. R. (1994) Lithologic and climatologic controls of river chemistry. *Geochim. Cosmochim. Acta* **58**(10), 2341–2359.

Brady P. V., and Gislason S. R. (1997) Seafloor weathering controls on atmospheric CO_2 and global climate. *Geochim. Cosmochim. Acta* **61**(5), 965–973.

Brady P. V., Dorn R. I., Brazel A. J., Clark J., Moore R. B., and Glidewell T. (1999) Direct measurement of the combined effects of lichen, rainfall, and temperature on silicate weathering. *Geochim. Cosmochim. Acta* **63**(19-20), 3293–3300.

Brantley S. L. (2003) Reaction kinetics of primary rock-forming minerals under ambient conditions. In *Treatise on Geochemistry, Surface and Ground Water, Weathering, and Soils* (ed. J. I. Drever, vol. 5.). Elsevier Pergamon, pp. 73–119.

Busenberg E., and Clemency C. V. (1976) The dissolution kinetics of feldspars at 25 °C and 1 atm CO_2 partial pressure. *Geochim. Cosmochim. Acta* **40**(1), 41–49.

Chadwick O. A., Derry L. A., Vitousek P. M., Huebert B. J., and Hedin L. O. (1999) Changing sources of nutrients during four million years of ecosystem development. *Nature* **397**(6719), 491–497.

Chadwick O. A., Gavenda R. T., Kelly E. F., Ziegler K., Olson C. G., Elliott W. C., and Hendricks D. M. (2003) The impact of climate on the biogeochemical functioning of volcanic soils. *Chem. Geol.* **202**(3-4), 195–223.

Cochran M. F., and Berner R. A. (1996) Promotion of chemical weathering by higher plants: field observations on Hawaiian basalts. *Chem. Geol.* **132**(1–4), 71–77.

Coenye T., Laevens S., Willems A., Ohlén M., Hannant W., Govan J. R. W., Gillis M., Falsen E., and Vandamme P. (2001) *Burkholderia fungorum* sp. nov. and *Burkholderia caledonica* sp. nov., two new species isolated from the environment, animals and human clinical samples. *Int. J. Syst. Evol. Microbiol.* **51**, 1099–1107.

Das A., and Krishnaswami S. (2006) Barium in Deccan basalt rivers; its abundance, relative mobility and flux. *Aquat. Geochem.* **12**(3), 221–238.

Das A., Krishnaswami S., and Kumar A. (2006) Sr and $^{87}Sr/^{86}Sr$ in rivers draining the Deccan Traps (India): implications to weathering, Sr fluxes, and the marine $^{87}Sr/^{86}Sr$ record around K/T. *Geochem. Geophys. Geosyst.* **7**(6). doi:10.1029/2005GC001081.

Daughney C. J., Rioux J.-P., Fortin D., and Pichler T. (2004) Laboratory investigation of the role of bacteria in the weathering of basalt near deep sea hydrothermal vents. *Geomicrobiol. J.* **21**, 21–31.

Dessert C., Dupré B., François L. M., Schott J., Gaillardet J., Chakrapani G., and Bajpai S. (2001) Erosion of Deccan Traps determined by river geochemistry: impact on the global climate and the $^{87}Sr/^{86}Sr$ ratio of seawater. *Earth Planet. Sci. Lett.* **188**, 459–474.

Dessert C., Dupré B., Gaillardet J., François L. M., and Allègre C. J. (2003) Basalt weathering laws and the impact of basalt weathering on the global carbon cycle. *Chem. Geol.* **202**(3-4), 257–273.

Drever J. I. (1994) The effect of land plants on weathering rates of silicate minerals. *Geochim. Cosmochim. Acta* **58**(10), 2325–2332.

Drever J. I., and Stillings L. L. (1997) The role of organic acids in mineral weathering. *Colloids Surfaces A* **120**(1-3), 167–181.

Dunfield K. E., and King G. M. (2005) Analysis of the distribution and diversity in recent Hawaiian volcanic deposits of a putative carbon monoxide dehydrogenase large subunit gene. *Environ. Microbiol.* **7**(9), 1405–1412.

Dupré B., Dessert C., Oliva P., Goddéris Y., Viers J., François L., Millot R., and Gaillardet J. (2003) Rivers, chemical weathering and Earth's climate. *CR Geosci.* **335**(16), 1141–1160.

Edwards K. J., Bach W., and Rogers D. R. (2003) Geomicrobiology of the ocean crust: a role for chemoautotrophic Fe–bacteria. *Biol. Bull.* **204**, 180–185.

Eick M. J., Grossl P. R., Golden D. C., Sparks D. L., and Ming D. W. (1996) Dissolution kinetics of a lunar glass simulant at 25 °C: The effect of pH and organic acids. *Geochim. Cosmochim. Acta* **60**(1), 157–170.

Finkel S. E. (2006) Long-term survival during stationary phase: evolution and the GASP phenotype. *Nat. Rev. Microbiol.* **4**, 113–120.

Fisk M. R., Giovannoni S. J., and Thorseth I. H. (1998) Alteration of oceanic volcanic glass: textural evidence of microbial activity. *Science* **281**, 978–980.

Garrels R. M., Thompson M. E., and Siever R. (1960) Stability of some carbonates at 25 °C and one atmosphere total pressure. *Am. J. Sci.* **258**, 439–453.

Gislason S. R., and Eugster H. P. (1987a) Meteoric water–basalt interactions. II: A field study in N.E. Iceland. *Geochim. Cosmochim. Acta* **51**(10), 2841–2855.

Gislason S. R., and Eugster H. P. (1987b) Meteoric water–basalt interactions. I: A laboratory study. *Geochim. Cosmochim. Acta* **51**(10), 2827–2840.

Gislason S. R., Veblen D. R., and Livi K. J. T. (1993) Experimental meteoric water–basalt interactions: characterization and interpretation of alteration products. *Geochim. Cosmochim. Acta* **57**(7), 1459–1471.

Gislason S. R., and Oelkers E. H. (2003) Mechanism, rates, and consequences of basaltic glass dissolution: II. An experimental study of the dissolution rates of basaltic glass as a function of pH and temperature. *Geochim. Cosmochim. Acta* **67**(20), 3817–3832.

Guidry M. W., and Mackenzie F. T. (2003) Experimental study of igneous and sedimentary apatite dissolution: control of pH, distance from equilibrium, and temperature on dissolution rates. *Geochim. Cosmochim. Acta* **67**(16), 2949–2963.

Gyaneshwar P., Kumar G. N., and Parekh L. J. (1998) Effect of buffering on the phosphate-solubilizing ability of microorganisms. *World J. Microb. Biot.* **14**, 669–673.

Hinsinger P., Barros O. N. F., Benedetti M. F., Noack Y., and Callot G. (2001) Plant-induced weathering of a basaltic rock: experimental evidence. *Geochim. Cosmochim. Acta* **65**(1), 137–152.

Ho C. S., Smith M. D., and Shanahan J. F. (1987) Carbon dioxide transfer in biochemical reactors. *Adv. Biochem. Eng. Biotechnol.* **35**, 83–127.

Holdren, Jr., G. R., and Berner R. A. (1979) Mechanism of feldspar weathering; I, Experimental studies. *Geochim. Cosmochim. Acta* **43**(8), 1161–1172.

Kalinowski B. E., Liermann L. J., Givens S., and Brantley S. L. (2000) Rates of bacteria-promoted solubilization of Fe from minerals: a review of problems and approaches. *Chem. Geol.* **169**(3–4), 357–370.

Köhler S. J., Harouiya N., Chaïrat C., and Oelkers E. H. (2005) Experimental studies of REE fractionation during water–mineral interactions: REE release rates during apatite dissolution from pH 2.8 to 9.2. *Chem. Geol.* **222**(3-4), 168–182.

Kraemer S. M. (2004) Iron oxide dissolution and solubility in the presence of siderophores. *Aquat. Sci.* **66**, 3–18.

Lerman A. (1979) *Geochemical Processes; Water and Sediment Environments*. John Wiley.

Lerman, A., and Wu, L. (in press) Kinetics of global geochemical cycles. In *Kinetics of Water–Rock Interaction* (eds. J. D. K. S. L. Brantley and A. F. White). Springer–Kluwer Publishers.

Li Y.-H. (2000) *A Compendium of Geochemistry, from Solar Nebula to the Human Brain*. Princeton University Press, Princeton, NJ.

Liermann L. J., Kalinowski B. E., Brantley S. L., and Ferry J. G. (2000) Role of bacterial siderophores in dissolution of hornblende. *Geochim. Cosmochim. Acta* **64**(4), 587–602.

Luce R. W., Bartlett R. W., and Parks G. A. (1972) Dissolution kinetics of magnesium silicates. *Geochim. Cosmochim. Acta* **36**(1), 35–50.

Lüttge A., and Conrad P. G. (2004) Direct observation of microbial inhibition of calcite dissolution. *Appl. Environ. Microbiol.* **70**(3), 1627–1632.

Morel F. M. M., and Hering J. G. (1993) *Principles and Applications of Aquatic Chemistry*. John Wiley.

Moulton K. L., and Berner R. A. (1998) Quantification of the effect of plants on weathering: studies in Iceland. *Geology* **26**(10), 895–898.

Moulton K. L., West J., and Berner R. A. (2000) Solute flux and mineral mass balance approaches to the quantification of plant effects on silicate weathering. *Am. J. Sci.* **300**, 539–570.

Neaman A., Chorover J., and Brantley S. L. (2005) Implications of the evolution of organic acid moieties for basalt weathering over geological time. *Am. J. Sci.* **305**(2), 147–185.

Oelkers E. H., and Schott J. (1998) Does organic acid adsorption affect alkali–feldspar dissolution rates? *Chem. Geol.* **151**(1–4), 235–245.

Oelkers E. H. (2001) General kinetic description of multioxide silicate mineral and glass dissolution. *Geochim. Cosmochim. Acta* **65**(21), 3703–3719.

Oelkers E. H., and Gislason S. R. (2001) The mechanism, rates and consequences of basaltic glass dissolution: I. An experimental study of the dissolution rates of basaltic glass as a function of aqueous Al, Si and oxalic acid concentration at 25 °C and pH = 3 and 11. *Geochim. Cosmochim. Acta* **65**(21), 3671–3681.

Oelkers E. H., and Schott J. (2001) An experimental study of enstatite dissolution rates as a function of pH, temperature, and aqueous Mg and Si concentration, and the mechanism of pyroxene/pyroxenoid dissolution. *Geochim. Cosmochim. Acta* **65**(8), 1219–1231.

Paces T. (1973) Steady-state kinetics and equilibrium between ground water and granitic rock. *Geochim. Cosmochim. Acta* **37**, 2641–2663.

Plummer L. N., and Mackenzie F. T. (1974) Predicting mineral solubility from rate data; application to the dissolution of magnesian calcites. *Am. J. Sci.* **274**(1), 61–83.

Pokrovsky O. S., Schott J., Kudryavtzev D. I., and Dupré B. (2005) Basalt weathering in Central Siberia under permafrost conditions. *Geochim. Cosmochim. Acta* **69**(24), 5659–5680.

Ramachandran S., Fontanille P., Pandey A., and Larroche C. (2006) Gluconic acid: properties, applications and microbial production. *Food Tech. Biotech.* **44**(2), 185–195.

Reyes I., Bernier L., Simard R. R., and Antoun H. (1999) Effect of nitrogen source on the solubilization of different inorganic phosphates by an isolate of *Penicillium rugulosum* and two UV-induced mutants. *FEMS Microbiol. Ecol.* **28**(3), 281–290.

Reysenbach A.-L., and Shock E. (2002) Merging genomes with geochemistry in hydrothermal ecosystems. *Science* **296**(5570), 1077–1082.

Rittman B. E., and McCarty P. L. (2000) *Environmental Biotechnology: Principles and Applications*. McGraw-Hill College.

Roberts J. A., Bennett P. C., González L. A., Macpherson G. L., and Milliken K. L. (2004) Microbial precipitation of dolomite in methanogenic groundwater. *Geology* **32**(4).

Rogers J. R., Bennett P. C., and Choi W. J. (1998) Feldspars as a source of nutrients for microorganisms. *Am. Mineral.* **83**(11–12, Part 2), 1532–1540.

Rogers J. R., and Bennett P. C. (2004) Mineral stimulation of subsurface microorganisms: release of limiting nutrients from silicates. *Chem. Geol.* **203**(1–2), 91–108.

Roos W., and Luckner M. (1984) Relationships between proton extrusion and fluxes of ammonium ions and organic acids in *Penicillium cyclopium*. *J. Gen. Microbiol.* **130**, 1007–1014.

Santelli C. M., Welch S. A., Westrich H. R., and Banfield J. F. (2001) The effect of Fe-oxidizing bacteria on Fe–silicate mineral dissolution. *Chem. Geol.* **180**(1–4), 99–115.

Sebat J. L., Colwell F. S., and Crawford R. L. (2003) Metagenomic profiling: microarray analysis of an environmental genomic library. *Appl. Environ. Microbiol.* **69**(8), 4927–4934.

Staudigel H., Chastain R. A., Yayanos A., and Bourcier W. (1995) Biologically mediated dissolution of glass. *Chem. Geol.* **126**(2), 147–154.

Staudigel H., Yayanos A., Chastain R., Davies G., Verdurmen E. A. T., Schiffman P., Bourcier R., and De Baar H. (1998) Biologically mediated dissolution of volcanic glass in seawater. *Earth Planet. Sci. Lett.* **164**(1–2), 233–244.

Stewart B. W., Capo R. C., and Chadwick O. A. (2001) Effects of rainfall on weathering rate, base cation provenance, and Sr isotope composition of Hawaiian soils. *Geochim. Cosmochim. Acta* **65**(7), 1087–1099.

Stumm W., and Morgan J. J. (1981) *Aquatic Chemistry; An Introduction Emphasizing Chemical Equilibria in Natural Waters*. John Wiley.

Sverdrup H. (1990) *The Kinetics of Base Cation Release Due to Chemical Weathering*. Lund University Press.

Taylor A. S., and Lasaga A. C. (1999) The role of basalt weathering in the Sr isotope budget of the oceans. *Chem. Geol.* **161**(1–3), 199–214.

Templeton A. S., Trainor T. P., Spormann A. M., Newville M., Sutton S. R., Dohnalkova A., Gorby Y., and Brown, Jr., G. E. (2003) Sorption versus biomineralization of Pb(II) within

Burkholderia cepacia biofilms. *Environ. Sci. Technol.* **37**, 300–307.

Thorseth I. H., Furnes H., and Heldal M. (1992) The importance of microbiological activity in the alteration of natural basaltic glass. *Geochim. Cosmochim. Acta* **56**(2), 845–850.

Thorseth I. H., Torsvik T., Furnes H., and Muehlenbachs K. (1995) Microbes play an important role in the alteration of oceanic crust. *Chem. Geol.* **126**(2), 137–146.

Torsvik T., Furnes H., Muehlenbachs K., Thorseth I. H., and Tumyr O. (1998) Evidence for microbial activity at the glass-alteration interface in oceanic basalts. *Earth Planet. Sci. Lett.* **162**(1–4), 165–176.

Ullman W. J., Kirchman D. L., Welch S. A., and Vandevivere P. (1996) Laboratory evidence for microbially mediated silicate mineral dissolution in nature. *Chem. Geol.* **132**(1–4), 11–17.

VanBriesen J. M., and Rittman B. E. (1999) Modelling speciation effects on biodegradation in mixed metal/chelate systems. *Biodegradation* **10**, 315–330.

Vandevivere P., Welch S. A., Ullman W. J., and Kirchman D. L. (1994) Enhanced dissolution of silicate minerals by bacteria at near-neutral pH. *Microb. Ecol.* **27**, 241–251.

Vitousek P. M., Kennedy M. J., Derry L. A., and Chadwick O. A. (1999) Weathering versus atmospheric sources of strontium in ecosystems on young volcanic soils. *Oecologia* **121**, 255–259.

Welch S. A., Barker W. W., and Banfield J. F. (1999) Microbial extracellular polysaccharides and plagioclase dissolution. *Geochim. Cosmochim. Acta* **63**(9), 1405–1419.

Welch S. A., and Ullman W. J. (1999) The effect of microbial glucose metabolism on bytownite feldspar dissolution rates between 5 °C and 35 °C. *Geochim. Cosmochim. Acta* **63**(19-20), 3247–3259.

Welch S. A., and Banfield J. F. (2002) Modification of olivine surface morphology and reactivity by microbial activity during chemical weathering. *Geochim. Cosmochim. Acta* **66**(2), 213–221.

Welch S. A., Taunton A. E., and Banfield J. F. (2002) Effect of microorganisms and microbial metabolites on apatite dissolution. *Geomicrobiol. J.* **19**(3), 343–367.

White A. F. (1995) Chemical weathering rates of silicate minerals in soils. In *Chemical Weathering Rates of Silicate Minerals* (eds. A. F. White and S. L. Brantley, vol. 31.). Mineralogical Society of America, pp. 407–458.

Wolff-Boenisch D., Gislason S. R., Oelkers E. H., and Putnis C. V. (2004) The dissolution rates of natural glasses as a function of their composition at pH 4 and 10.6, and temperatures from 25 to 74 °C. *Geochim. Cosmochim. Acta* **68**(23), 4843–4858.

Wolff-Boenisch D., Gislason S. R., and Oelkers E. H. (2006) The effect of crystallinity on dissolution rates and CO_2 consumption capacity of silicates. *Geochim. Cosmochim. Acta* **70**(4), 858–870.

Wollast R. (1967) Kinetics of the alteration of K-feldspar in buffered solutions at low temperature. *Geochim. Cosmochim. Acta* **31**(4), 635–648.

Wu L., Chen H.-C., Jacobson A. D., and Hausner M. (2006) Microbially mediated dissolution of granite and fluorapatite. *International IWA Conference on Biofilm Systems VI*.

Associate editor: Eric H. Oelkers